5-10-2017

The FOXO Transcription Factor Controls Insect Growth and Development by Regulating Juvenile Hormone Degradation in the Silkworm, *Bombyx mori*

Baosheng Zeng
Chinese Academy of Sciences, China

Yuping Huang
Chinese Academy of Sciences, China

Jun Xu
Chinese Academy of Sciences, China

Takahiro Shiotsuki
Institute of Agrobiological Sciences, Japan

Hua Bai
Iowa State University

See next page for additional authors

The FOXO Transcription Factor Controls Insect Growth and Development by Regulating Juvenile Hormone Degradation in the Silkworm, *Bombyx mori*

Authors

Baosheng Zeng, Yuping Huang, Jun Xu, Takahiro Shiotsuki, Hua Bai, Subba Reddy Palli, Yongping Huang, and Anjiang Tan

The FOXO transcription factor controls insect growth and development by regulating juvenile hormone degradation in the silkworm, *Bombyx mori*

Received for publication, January 22, 2017, and in revised form, May 8, 2017 Published, Papers in Press, May 10, 2017, DOI 10.1074/jbc.M117.777797

Baosheng Zeng[‡§], Yuping Huang[‡], Jun Xu[‡§], Takahiro Shiotsuki[¶], Hua Bai[‖], Subba Reddy Palli[**], Yongping Huang[‡], and Anjiang Tan[‡1]

*From the [‡]Key Laboratory of Insect Developmental and Evolutionary Biology, Institute of Plant Physiology and Ecology, Shanghai Institutes for Biological Sciences, Chinese Academy of Sciences, Shanghai 200032, China, the [§]University of Chinese Academy of Sciences, Beijing 100049, China, the [¶]National Agriculture and Food Research Organization, Institute of Agrobiological Sciences, Division of Insect Science, 1-2 Owashi, Tsukuba, Ibaraki 305-8634, Japan, the [‖]Department of Genetics, Development, and Cell Biology, Iowa State University, Ames, Iowa 50011, and the **Department of Entomology, University of Kentucky, Lexington, Kentucky 40546-0091*

Edited by Joel Gottesfeld

Forkhead box O (FOXO) functions as the terminal transcription factor of the insulin signaling pathway and regulates multiple physiological processes in many organisms, including lifespan in insects. However, how FOXO interacts with hormone signaling to modulate insect growth and development is largely unknown. Here, using the transgene-based CRISPR/Cas9 system, we generated and characterized mutants of the silkworm *Bombyx mori* FOXO (*BmFOXO*) to elucidate its physiological functions during development of this lepidopteran insect. The *BmFOXO* mutant (FOXO-M) exhibited growth delays from the first larval stage and showed precocious metamorphosis, pupating at the end of the fourth instar (trimolter) rather than at the end of the fifth instar as in the wild-type (WT) animals. However, different from previous reports on precocious metamorphosis caused by juvenile hormone (JH) deficiency in silkworm mutants, the total developmental time of the larval period in the FOXO-M was comparable with that of the WT. Exogenous application of 20-hydroxyecdysone (20E) or of the JH analog rescued the trimolter phenotype. RNA-seq and gene expression analyses indicated that genes involved in JH degradation but not in JH biosynthesis were up-regulated in the FOXO-M compared with the WT animals. Moreover, we identified several FOXO-binding sites in the promoter of genes coding for JH-degradation enzymes. These results suggest that FOXO regulates JH degradation rather than its biosynthesis, which further modulates hormone homeostasis to control growth and development in *B. mori*. In conclusion, we have uncovered a pivotal role for FOXO in regulating JH signaling to control insect development.

Insect growth and development are intricately modulated by many conserved signaling pathways. The insulin/insulin-like growth factor signaling (IIS)[2] and target of rapamycin pathways regulate growth rate via nutrition and immunity levels (1, 2). Growth periods, including molting and metamorphosis, are governed by ecdysteroid and juvenile hormone (JH) (3, 4). Previous studies have shown that ecdysone synthesis is regulated by IIS and target of rapamycin signaling, whereas IIS is antagonized by ecdysteroids (5–7). In *Drosophila melanogaster* mutations to genes in the IIS not only perturb growth and result in smaller body size (8–10) but also alter JH biosynthesis (11). The cross-talk between IIS and hormones indicates the complexity of regulation in insect development. However, the detailed mechanism of how IIS interacts with insect developmental hormones remains largely unknown.

As the major terminal transcription factor of IIS and the target of protein kinase B (PKB/Akt), the forkhead box O (FOXO) (12) plays multiple roles in many cellular and physiological processes (13). FOXO has been identified as the key factor in limiting longevity in worms (*daf-16*) and flies (*dFOXO*) (14–17). The overexpression of *dFOXO* during early larval stages inhibited larval growth (18) and showed reduced body size when expressed in the third instar larvae (19). The ectopic expression of *dFOXO* in specific tissues (*i.e.* eye or wing) also led to characteristic phenotypes with reduced cell size and cell number that could partially be rescued by the co-expression of upstream insulin signaling components (19). Furthermore, as IIS-mediated growth control is FOXO-dependent, the loss-of-function of FOXO also results in delayed adult development time and smaller size (20). In contrast to *daf-16*, the multitude of phenotypes caused by the reduction in IIS are not completely suppressed in the absence of FOXO, and only the increase in lifespan extension phenotype was blocked by the removal of *dFOXO* in *D. melanogaster* (20). Although the regulatory networks of IIS and FOXO are well understood, it remains unclear

This work was supported by Strategic Priority Research Program of Chinese Academy of Sciences Grant XDB11010600, National Basic Research Program of China Grant 2015CB755703, National Science Foundation of China Grants 31420103918 and 31530072, and Chinese Academy of Sciences Grant KJZD-EW-L12-02. The authors declare that they have no conflicts of interest with the contents of this article.

This article contains supplemental Tables S1 and S2 and Figs. S1–S9.

[1] To whom correspondence should be addressed. Tel.: 86-021-54924046; E-mail: ajtan01@sibs.ac.cn.

[2] The abbreviations used are: IIS, insulin/insulin-like growth factor signaling; FOXO, forkhead box O; JH, juvenile hormone; PG, prothoracic glands; 20E, 20-hydroxyecdysone; JHE, juvenile hormone esterase; JHEH, juvenile hormone epoxidase hydrolase; JHDK, juvenile hormone diol kinase; CA, corpora allata.

how FOXO interacts with hormone signaling to mediate growth and development.

Most FOXO functional analyses in *Drosophila* have focused on its roles in the regulation of IIS-mediated growth control (1, 2). The effects of JH on growth rate are dependent on FOXO (4). Recent studies have implicated FOXO in the regulation of JH metabolism but did not further explore the underlying mechanisms (22, 23). Nevertheless, as *Drosophila* exhibits relatively short larval development and body size, there are only a few reports concerning the precise function of FOXO in the modulation of the metamorphic transition that could be explored in other insects, such as the lepidopteran model insect *Bombyx mori*, which exhibits a longer developmental time and a larger body size. In *B. mori*, *BmFOXO* is highly expressed in the fat body and could be induced by 20E to promote lipolysis. The down-regulation of *BmFOXO* during the fourth larval instar using RNAi partially delayed the molting process (24). However, the comprehensive functions of FOXO in *B. mori* have yet to be revealed. Recent advances in genetic manipulation techniques, such as transgenesis and genome editing tools (25, 26), have provided promising approaches for dissecting functions of genes such as *BmFOXO*.

Here, we elucidated how FOXO interacts with hormone signaling to regulate growth and metamorphosis in *B. mori* by knocking out *BmFOXO* using the transgene-based CRISPR/Cas9 system. BmFOXO mutants showed a significant growth delay from the second larval instar and skipped the last molt, resulting in precocious metamorphosis after only four larval instars (trimolter), although the entire developmental time of the larval instar was comparable with that of WT animals. The hormone titers (both JH and 20E) were lower in mutants, and the phenotypic defects could be rescued by applying either 20E or JH analogs. Intriguingly, the transcriptome analysis revealed that the genes coding for JH metabolizing but not biosynthesis enzymes were up-regulated in mutants. We confirmed that FOXO binds to the response elements present in the promoter of these genes. Our results revealed a novel mechanism by which FOXO interacts with the JH degradation pathway to regulate growth and development in silkworms.

Results

Generation of BmFOXO mutants using the transgenic CRISPR/Cas9 system

To generate FOXO mutants, we used a binary transgenic CRISPR/Cas9 system that has been described in our previous publication (27). Two guide RNAs (sgRNA) targeting exons 2 and 3 coding for the majority of forkhead domain, were selected (supplemental Fig. S1*A*). We constructed two *piggyBac* transposon-based transformation plasmids expressing Cas9 protein or the FOXO-sgRNAs (supplemental Fig. S1*B*). The *nanos* promoter was used to specifically express Cas9 protein in the germline (28, 29), whereas sgRNAs were expressed under control of the ubiquitous U6 promoter, as described previously (30). Transgenic animals carrying *nos-Cas9* or *U6-FOXO-sgRNA* were fully viable and fertile, indicating that the accumulation of neither Cas9 nor FOXO-sgRNA alone had a deleterious effect on silkworm physiology. We crossed the *nos*-Cas9 and U6-FOXO-sgRNA lines to obtain founder offspring that specifically express the active Cas9-sgRNA complex in the germline, resulting in mutations at targeted genomic loci of the *BmFOXO* gene (supplemental Fig. S1*B*). We investigated the *BmFOXO* mutation in different tissues (brain, fat body, silk gland, epidermis, mid-gut, ovary, and testis) and found that two CRISPR targeting sites (*BmFOXO*-s1 and *BmFOXO*-s2) were disrupted effectively in all tissues tested (supplemental Fig. S1*C*).

The somatic mutation events were evaluated using polymerase chain reaction (PCR) analysis and subsequent sequencing of the targeted genomic loci. The sequencing results identified various deletion mutations at two sgRNA targets and deletions ranging from 2 to 64 bp, indicating that successful mutations were induced using the transgenic CRISPR system (supplemental Fig. S1*D*). Western blots showed a significant decrease in the levels of the BmFOXO protein in the fat body (where *BmFOXO* is dominantly expressed) in the mutants (supplemental Fig. S1*E*). These results revealed successful disruption of the *BmFOXO* gene *in vivo*.

Precocious metamorphosis in BmFOXO mutants

BmFOXO mutants showed no deleterious effects during embryonic development. However, unlike WT larvae that molt four times prior to metamorphosis, the mutant larvae grew slower and molted only three times (Fig. 1*A*). The mutants showed significant growth delay from the first to the third larval stage when compared with the WT animals (Figs. 1*A* and supplemental Fig. S2). However, both the mutants and WT animals reached similar body sizes before entering the fourth larval stage (L4). Interestingly, unlike the WT animals that entered the final (fifth) instar stage after the fourth molting and ecdysis, 78% of FOXO mutants ($n = 80$) did not undergo the fourth molt prior to the larval-pupal metamorphosis (Fig. 1*A*).

The time span of the fourth instar mutants (120 h) is longer than that of the fourth (72 h) and fifth instar (84 h) WT animals (Fig. 1*A*). The silk glands in the mutants have undergone premature development and the accumulation of carotenoids (which turned the middle silk gland yellow), a character of mature silk glands were detected from the L4D4. The mature silk glands occurred 72 h earlier than in WT animals (supplemental Fig. S3). The mutant body size (including wandering larvae, pupae and adults) was significantly reduced. The mutant silkworms were approximately half the weight of WT animals (Fig. 1, *B* and *C*, supplemental Figs. S4 and S5). However, pupation and eclosion processes were normal (supplemental Fig. S6) and female mutants were fully fertile but laid fewer eggs (supplemental Fig. S7).

Because FOXO is a terminal transcription factor in IIS, expressions of genes known to play critical roles in IIS were determined by quantitative PCR in WT and *BmFOXO* mutants. The results showed that the expression of the insulin receptor (*InR*) gene was reduced by 86%, whereas the serine/threonine kinase (*Akt*) and 4E-binding protein (4EBP) were up-regulated in mutants when compared with their expression in WT (Fig. 1*D* and supplemental S2*B*). These results suggest that the loss of FOXO function perturbed IIS.

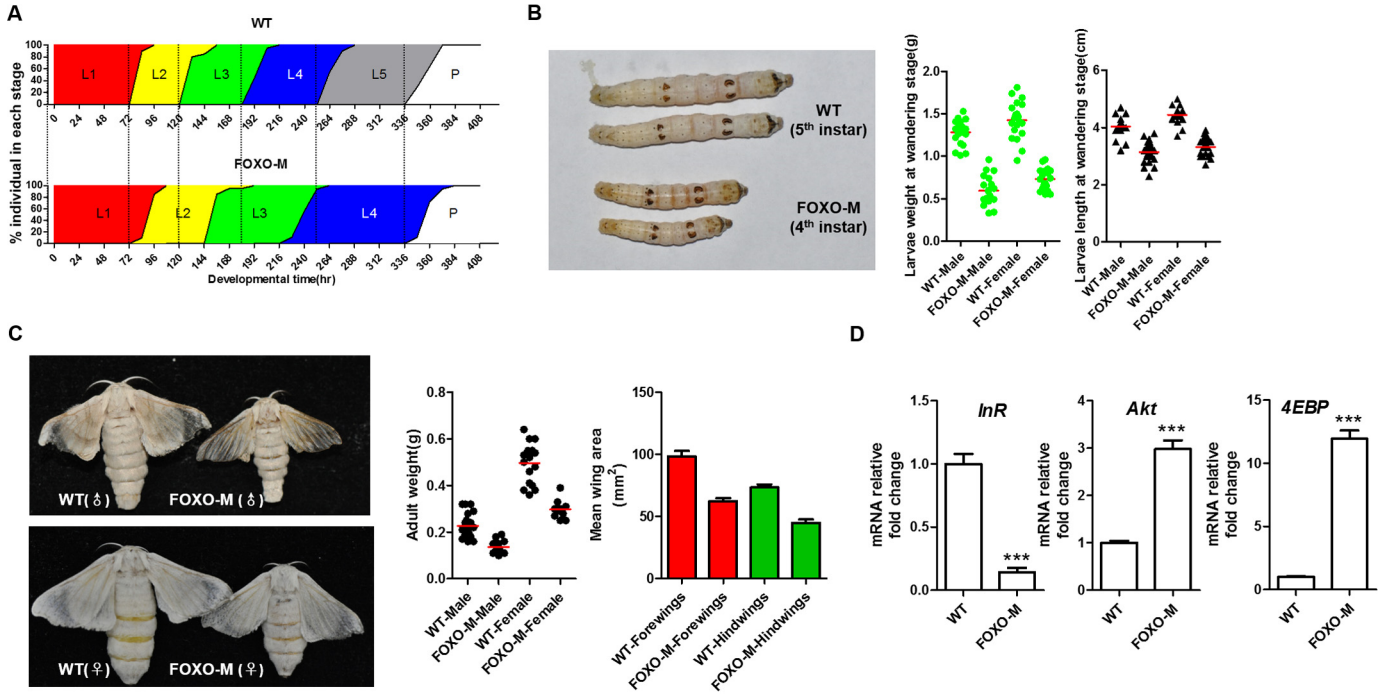

Figure 1. Developmental defects and reduced body size in FOXO mutants. *A,* the stages of larval development in WT and mutants (FOXO-M) (*L1*, first instar; *L2*, second instar; *L3*, third instar; *L4*, fourth instar; *L5*, fifth instar; *P*, pupae). L1-P stages are marked in *red*, *yellow*, *green*, *blue*, *gray*, and *white* sequentially through the developmental timeline. The *dashed lines* at time points 72, 120, 180, 252, and 336 h indicate the transition checkpoint of wild-type larvae. The *curve* between different stages shows the molting ratio. *B,* the size of wandering larvae of WT and FOXO-M. Two WT and FOXO-M larvae were photographed during the second day after larvae stopped feeding. The *right* graph show the male and female larval weight and body length at the wandering stage. *C,* adult body weight and wing area were reduced in mutants. The *left* graph shows the pictures of WT and FOXO-M adults (male on the top and female on the bottom). Both male and female adult weights were calculated ($n = 20$), the *red line* represents the average weight. The average areas of forewings and hindwings were shown as *red* and *green bars*, respectively. *D,* the mRNA levels of insulin signaling genes in the fat body of mutants. The relative InR, Akt, and 4EBP mRNA levels on the third day of fourth instar (L4D3) larvae were determined using RP49 as a control. The data are shown as the mean ± S.D. ($n = 3$). ***, $p < 0.001$ according to Student's *t* test.

Defective ecdysone signaling in BmFOXO mutants

The ecdysteroid titers increase during the larval-larval or larval-pupal transitions to initiate molting or metamorphosis (31). We measured the ecdysteroid levels in hemolymph on the second and third days of the fourth larval stage (L4D2 and L4D3). The results showed that ecdysteroid levels in the mutants decreased ~45 and 28% on L4D2 and L4D3, respectively, when compared with their levels in WT animals (Fig. 2*A*), suggesting that lower ecdysteroid titers in mutants might be responsible for their failure to undergo a fourth molt. Moreover, injection of 20E into the L4D3 mutant larvae caused 75% of them to molt into the fifth larval instar by 60 h after injection (Fig. 2*B* (*b* and *b*″) and *C*). Twenty-five percent of the 20E-injected mutant larvae were either partially rescued or died (*b*‴ in Fig. 2*B* and supplemental Fig. S8). The successfully rescued larvae went through a longer fifth larval stage and reached a larger pupal body size. These results showed that the application of 20E could turn trimolters back to tetramolters in most FOXO mutants suggesting that lower levels of ecdysteroids during L4 could be a reason for the trimolter phenotype observed in these animals.

We then investigated the expression levels of genes known to be involved in ecdysone action. Significantly lower levels of *E75*, hormone receptor 3 (*HR3*), and ecdysone receptor isoform A (*EcRA*) mRNA were detected on L4D2 and L4D3 in the mutants when compared with their levels in WT (Fig. 3, *A*–*C*). Furthermore, we determined the expression pattern of the *HR3* gene from L3D1 to wandering stage in WT and mutants and found that *HR3* mRNA levels were significantly lower in mutants when compared with its levels in WT during the L4 to L5 transition. These data suggest confirmation of the lower levels of ecdysteroids during this period and the reduction in ecdysteroid titers may be responsible for trimolter phenotype observed (Fig. 3*D*). No significant expression changes in the *broad* gene were detected (supplemental Fig. S6*D*), *broad* plays an essential role in pupal commitment (3), indicating that loss of FOXO did not interfere with the larval-pupal transition. Our results suggest that the expression of genes from ecdysone signaling was suppressed in FOXO mutants and contributed to the appearance of trimolter phenotype.

We also investigated the changes in expression genes coding for the major key enzymes in ecdysteroid biosynthesis (in the prothoracic glands, PG) and metabolism pathways (in the fat body). The changes in expression of ecdysteroid biosynthesis genes in the PG on L4D3 were variable and gene-dependent. *Neverland* (*Nvd*) and *Disembodied* (*Dib*) were up-regulated by 3.63- and 1.73-fold, respectively, whereas *Spook* (*Spo*), *Phantom* (*Phm*), and *Shade* (*Shd*) were down-regulated by 1.89-, 4.76-, and 1.92-fold, respectively (Fig. 3*F*). The expression of ecdysone oxidase (*EO*) was also significantly reduced (Fig. 3*E*). The expression pattern of ecdysteroid biosynthesis and metabolism genes suggest that *BmFOXO* depletion may have disrupted ecdysteroid signaling as well as ecdysteroid biosynthesis and metabolism.

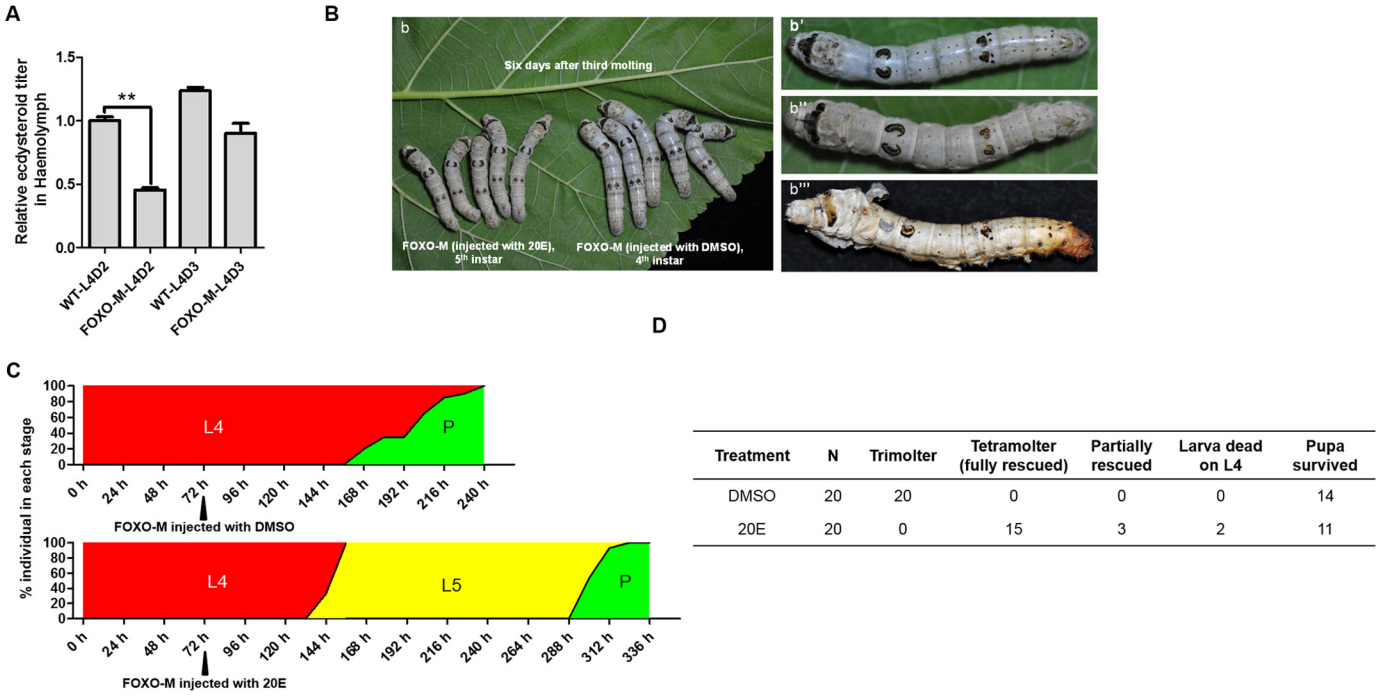

Treatment	N	Trimolter	Tetramolter (fully rescued)	Partially rescued	Larva dead on L4	Pupa survived
DMSO	20	20	0	0	0	14
20E	20	0	15	3	2	11

Figure 2. The ecdysteroid titers and 20E rescue of trimolter. *A,* measurement of relative 20E titers in the hemolymph on L4D2 and L4D3 of WT and FOXO-M. Hemolymph was collected from ~10 larvae, and the pooled sample was used to determine 20E titers. **, $p < 0.005$ according to Student's *t* test. *B, b,* FOXO mutant larvae injected with 20E (*left*) or DMSO (*right*) on the sixth day after the third molt ($n = 20$). FOXO-M injected with 20E reached the fifth instar, whereas those injected with DMSO remained in the fourth instar; *b'*, one larva from the DMSO-injected group (fourth instar); b'', one larva from 20E-injected group (fifth instar); b''', one larva from 20E-injected group, which partially recovered molting but failed to reach the next stage. *C,* the development of two groups in later stages. L4-P stages are marked in *red*, *yellow*, and *green*, respectively. The *curve* between different stages shows the transition ratio. The *dark filled triangles* indicate the time points when 20E or DMSO was injected. *D*, summary of 20E rescue. Twenty mutant larvae were treated in each group.

Activation of the JH metabolism pathway in BmFOXO mutants

Because precocious metamorphosis is a typical JH-deficient phenotype in *B. mori* (32, 33), we hypothesized that FOXO depletion might have affected JH signaling. We investigated the JH titers during the L4 of WT and FOXO-M and found that JH I in the hemolymph collected from mutants was reduced significantly to undetectable levels (Fig. 4*A*). Also, application of the JH analog, methoprene, to the newly molted fourth instar mutant larvae resulted in a rescue and all treated mutants having undergone a fourth molt (Fig. 4, *B* and *C*). The acetone-treated mutant larvae skipped the fifth instar and became pupae at 144 h after the third molt, whereas the rescued larvae have undergone the fourth molt at 132 h after methoprene application and began to spin at around 168 h after ecdysis (Fig. 4*D*). The body size of rescued larvae was similar to WT animals. Taken together, these data suggest that *BmFOXO* depletion affects titers and action of both JH and 20E, the two most important hormones that regulate molting and metamorphosis. Because of changes in hormone titers and action, the FOXO mutants have undergone three molts, whereas WT animals undergo four molts.

To explore the molecular basis for the phenotypic effects observed, we performed differential gene expression analysis by sequencing the fat body dissected from the mutant and WT animals and detected numerous differentially expressed genes between mutants and WT animals. These genes were primarily involved in cellular and metabolic processes, and binding and catalytic activities according to GO functional classification (supplemental Fig. S9, *A* and *B*). There are 4666 genes down-regulated, and only 357 genes were up-regulated in mutants when compared with their expression in WT animals (supplemental Fig. S9, *C* and *D*). Interestingly, the primary JH degradation pathway genes, including juvenile hormone esterase (JHE), juvenile hormone epoxidase hydrolase (JHEH), and juvenile hormone diol kinase (JHDK), were highly up-regulated in mutants (supplemental Table S1). We confirmed the activation of these three genes in the fat body using quantitative PCR and found that all three genes were up-regulated on L4D3 (~107-fold increase for JHE, 6-fold increase for JHEH, and 3-fold increase for JHDK) (Fig. 5*B*). In contrast, on L4D2, only JHE showed a significant up-regulation (~19-fold increase). Also, JHE enzymatic activity in the hemolymph was much higher in the mutants than that in WT; the average JHE enzymatic activity was 4.45- and 3.92-fold high in mutants on L4D2 and L4D3, respectively, when compared with that in WT (Fig. 5*A*). We further explored the JHE expression pattern from the third instar until the wandering stage and observed that JHE mRNA levels are higher during each larval molt, particularly in the later fourth instar stage suggesting a dominant role of JHE overexpression in trimolter phenotype (Fig. 5*C*).

The lower expression levels of the key genes involved in JH signaling: *Kr-h1α* and *Kr-h1β* during third instar to wandering stage were detected in *BmFOXO* mutants when compared with their expression in WT (Fig. 5, *D* and *E*). In contrast, there is no significant difference in the expression of genes coding for two key enzymes that act at the final steps of the JH biosynthesis pathway, epoxidase (*CYP15C1*) and JHA methyltransferase (*JHAMT*) in corpora allata (CA) (Fig. 5*F*). These data suggest

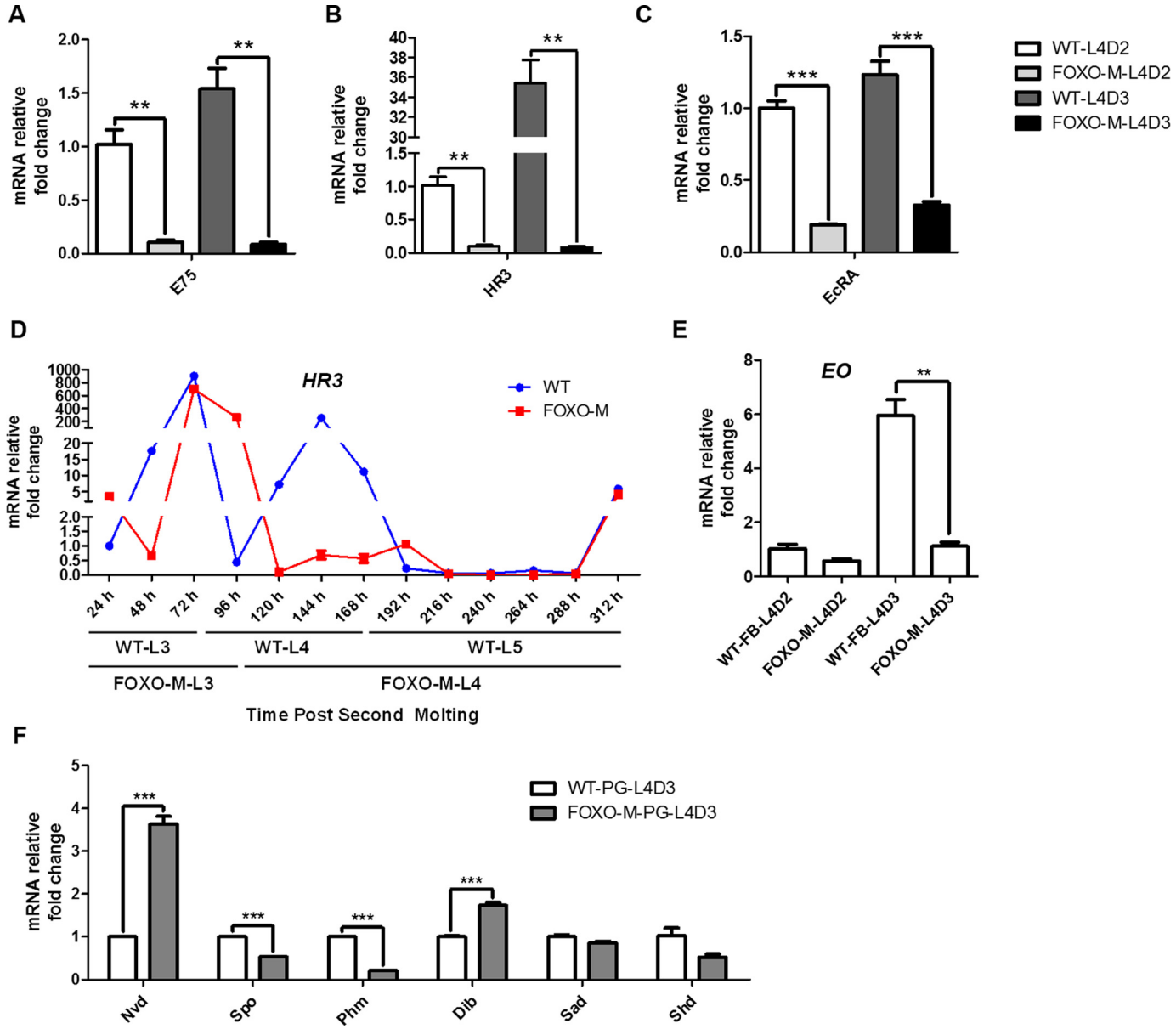

Figure 3. Expression differences of ecdysone pathway genes in mutants. *A–C*, reduction in mRNA levels of *E75*, *EcRA*, and *HR3* in the fat body. The *bars* with different colors in *A-C* represent the following: *white bar*, L4D2 in WT; *pale gray bar*, L4D2 in FOXO-M; *dark gray bar*, L4D3 in WT; and *black bar*, L4D3 in FOXO-M. *D*, the expression pattern of *HR3* in fat body (*FB*) from the third instar to wandering stage. The *x* axis represents the time post second molt, and *black lines below* the time line show different larval developmental stages in WT and FOXO-M. *E*, EO expression in the fat body from WT and FOXO-M on L4D2 and L4D3. The relative mRNA levels were normalized using RP49 was as a control. The expression level of genes in L4D2 was set as 1. *F*, expression change of the genes involved in the ecdysone biosynthesis pathway in PG on L4D3. Six genes were investigated: *Nvd*, *Spo*, *Phm*, *Dib*, *Sad*, and *Shd*. **, $p < 0.005$; ***, $p < 0.001$ according to Student's *t* test.

that *BmFOXO* depletion activated the JH degradation pathway but did not inhibit the JH biosynthesis pathway, which is different from the previous studies in *Drosophila* (20).

Identification of BmFOXO-binding sites in the promoter of genes coding for JH-metabolizing enzymes

As a terminal transcription factor of IIS, FOXO is known to bind to the conserved binding site (GTTTYAA (Y = T or C)) present in the promoters of many genes and regulate their expression (34). We searched 2-kb regions in the promoters of *JHE*, *JHEH*, and *JHDK* to identify potential binding sites for FOXO (Fig. 6*A*). Two potential FOXO-binding sites in the promoter regions of *JHE* and *JHDK* and one binding site in the *JHEH* promoter were identified (Fig. 6*A*). To examine whether FOXO can bind to these sites, we performed an electrophoretic mobility shift assay (EMSA) using purified His-tagged FOXO protein (Fig. 6, *B–D*).

We amplified an ~200 bp flanking sequence around the binding sites and labeled it with Cy5, followed by incubation with FOXO protein and resolved by gel electrophoresis. As shown in Fig. 6, FOXO bound to these predicted binding sites (Fig. 6, *B–D*). The competition experiments confirmed the specificity of FOXO binding. Depletion of *BmFOXO* induced the expression of genes coding for JH degradation enzymes suggesting that FOXO is likely involved in repression of JH degradation genes, and FOXO mutation eliminated this suppression

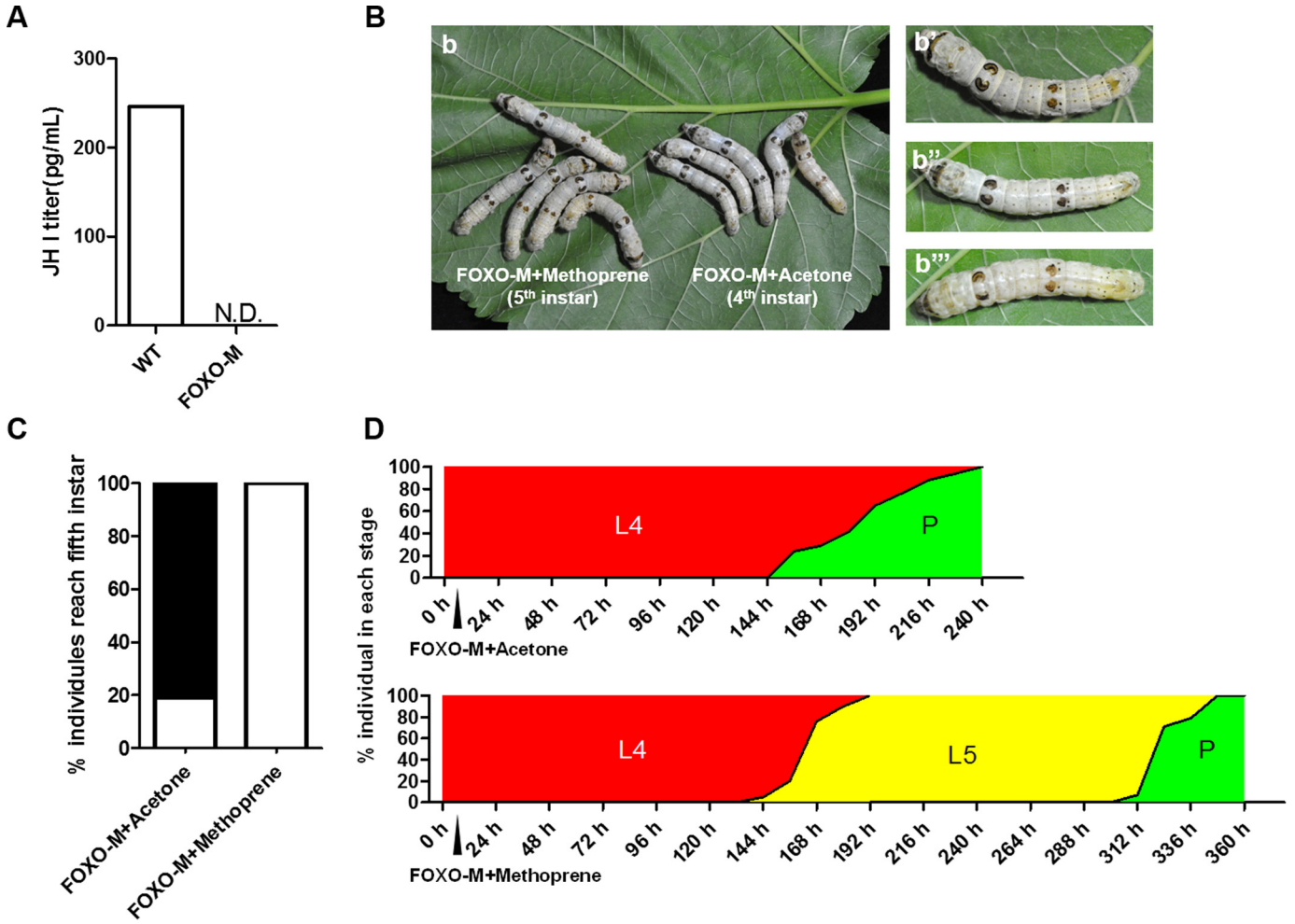

Figure 4. Trimolter larvae were fully rescued using the JH analog. *A,* measurement of the JHI titer in the hemolymph collected from larvae on the second day of the fourth instar (L4D2) of WT and FOXO-M. Hemolymph was collected from ~10 larvae, and the pooled samples were analyzed. JHI was undetected in the hemolymph of FOXO-M. *B,* FOXO-M larvae on the sixth day (~144 h) after application of methoprene or acetone (as a control). *b,* five individuals from different experimental groups. The group treated with methoprene (*FOXO-M + Methoprene*) molted into the fifth instar, whereas the other group treated with acetone (*FOXO-M + Acetone*) remained in the fourth instar. *b'*, one larva from the methoprene-treated group transformed into the fifth instar after 144 h. *b''*, one larva from the acetone-treated group remained in the fourth instar after 144 h. *b'''*, one larva in the acetone-treated group reached the wandering stage after 144 h. *C,* ratio of individuals reaching the fifth instar in two groups ($n = 20$). The *white section of the bar* represents individuals that reached the fifth instar (tetramolter), and the *black section* shows trimolter larvae. All individuals from the methoprene-treated group (100%) transitioned to the fifth instar, whereas only 20% in the acetone-treated group transitioned to this stage. *D*, the later stages of larval development in the two groups. L4-P stages are indicated in *red*, *yellow*, and *green*. The *curve* between different stages shows the transition ratio. The *dark-filled triangle* shows the time points when acetone or methoprene was applied.

effect, resulting in activation of these genes to accelerate JH degradation.

Discussion

In the present study, using a transgenic CRISPR/Cas9-derived somatic mutagenesis system, we showed that FOXO depletion affected growth and development as well as ecdysteroid and JH signaling in *B. mori*. Comparative analyses of growth and development in FOXO mutants and WT animals led to three major findings. First, the depletion of *BmFOXO* induced growth delay and precocious metamorphosis. Second, *BmFOXO* directly modulated the JH degradation pathway rather than the biosynthesis and thus perturbed the ecdysone homeostasis. Third, in contrast to typical JH-deficient mutants reported in previous studies (3, 32), *BmFOXO* depletion showed more complex phenotypes, suggesting *BmFOXO* as the nexus mediating the intimate link between various biological processes (Fig. 7).

Previous studies in *B. mori* suggested that embryonic growth and morphogenesis are independent of JHs, and precocious metamorphosis was induced after the second larval stage in the absence of JH or JH signaling (32). Also, the *nm-g* mutant in *Bombyx* reduced the ecdysteroid titer and induced larval arrest primarily during the first instar, suggesting a role for ecdysteroid during the early larval development (35). The growth delay in *BmFOXO* mutants initiated during the first larval instar was different from that in JH- or 20E-deprivation mutants, indicating that insulin signaling but not JH or 20E signaling play the dominant role in regulation of the early larval status in *B. mori.*

An intriguing finding in the present study is the emergence of the trimolter in FOXO mutants. The mutants took 36 h longer to reach the fourth larval stage, and spent 36 h shorter time than

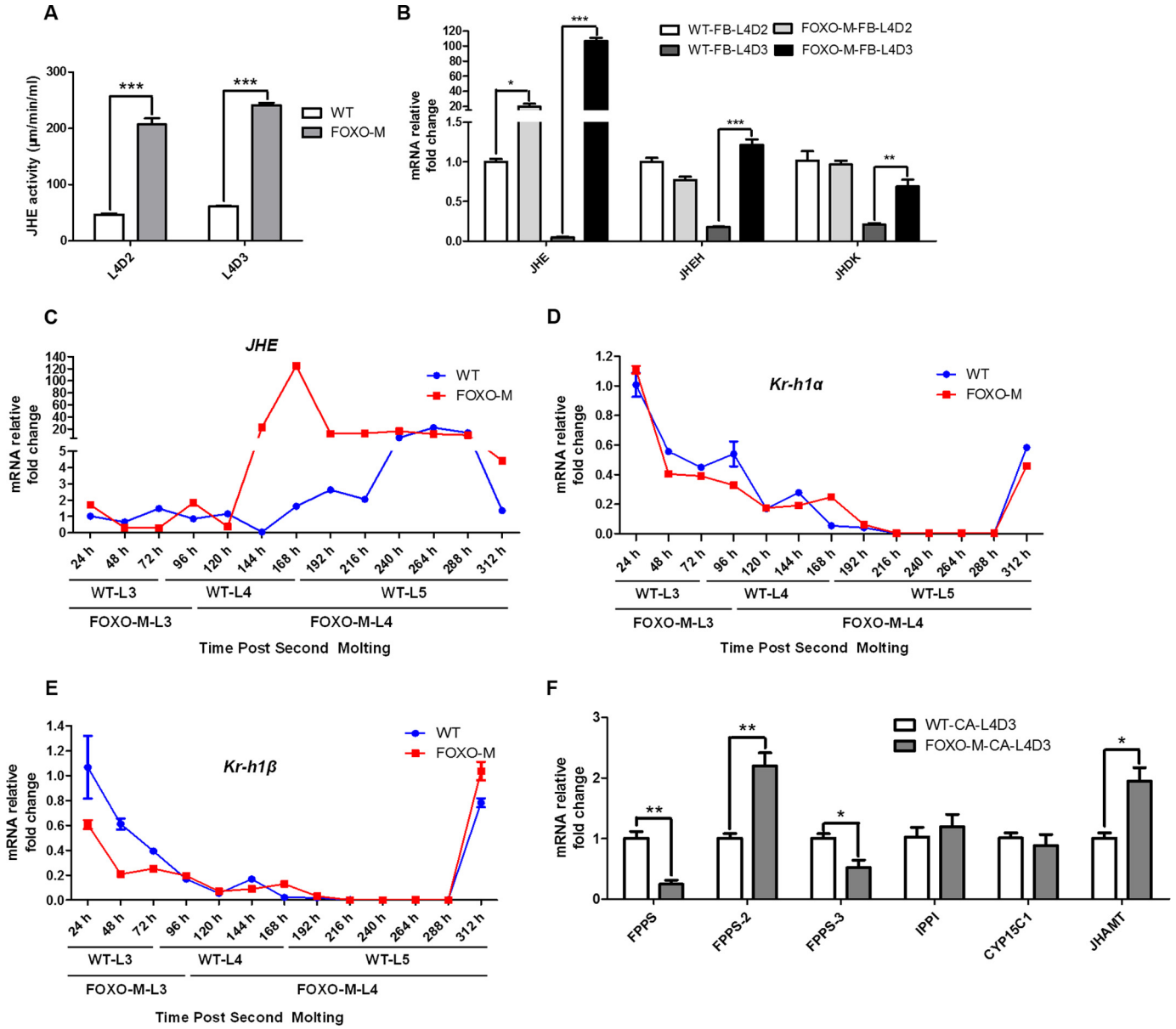

Figure 5. Activation of JH degradation rather than biosynthesis genes results in JH titer reduction. *A,* JHE enzymatic activity in the hemolymph was measured in the WT and FOXO-M during the fourth instar. The JHE activity in mutants (241.227 μm/min/ml) was 3-fold higher than that in the WT (61.495 μm/min/ml). *B,* relative expression of genes coding for JH degradation and synthesis enzymes in the fat body (*FB*). The expression changes of three significant genes in JH degradation: *JHE*, *JHEH*, and *JHDK* in L4D2 and L4D3 are shown. *White bar*, FB of WT on L4D2; *pale gray bar*, FB of FOXO-M on L4D2; *dark gray bar*, FB of WT on L4D3; *black bar,* FB of FOXO-M on L4D3. *C–E,* the expression patterns of *JHE*, *Kr-h1*α, and *Kr-h1*β in FB from third instar to wandering stage. The *x* axis represents the time post second molt, and *black lines below* the time line show different larval developmental stages in WT and FOXO-M. *F,* expression differences of several important genes coding for enzymes in JH biosynthesis, *FPPS*, *FPPS-2*, *FPPS-3*, *IPPI*, *CYP15C1*, and *JHAMT* in CA were investigated. The expression of all genes was normalized using RP49 as a control. The *bars* in *C* represent the following: *white bar,* CA of WT on L4D3; *gray bar*, CA of FOXO-M on L4D3. *, $p < 0.05$; **, $p < 0.005$; ***, $p < 0.001$ according to Student's *t* test.

the total developmental times of L4 and L5 in WT insects. Although the mutants experienced only four larval stages, the entire larval development period was not significantly different between WT and FOXO-M. The ecdysteroid titer was lower in the mutants, and the expression levels of ecdysone biosynthesis and degradation genes were affected. The phenotypic defects could be partially rescued by 20E application, suggesting the partial involvement of ecdysone action in FOXO mutants. Moreover, the *BmFOXO* trimolter mutants completely skipped the fourth molt without any deleterious physiological effects, molting defects, or lethality, indicating that reduced ecdysone synthesis and action are not the main reasons for the trimolter phenotype observed.

Furthermore, we detected a significant reduction in JH titers in mutants and fully rescued the trimolter to tetramolter by application of the JH analog, demonstrating the dominant role of JH. RNA-seq analysis, quantitative PCR, and EMSA experiments showed that activation of JH degradation in FOXO mutants may be the primary factor contributing to this phenotype. Previous studies showed that the effects of JH on the growth rate depend on FOXO (4, 22), and our data revealed a direct connection between FOXO, which is involved the IIS

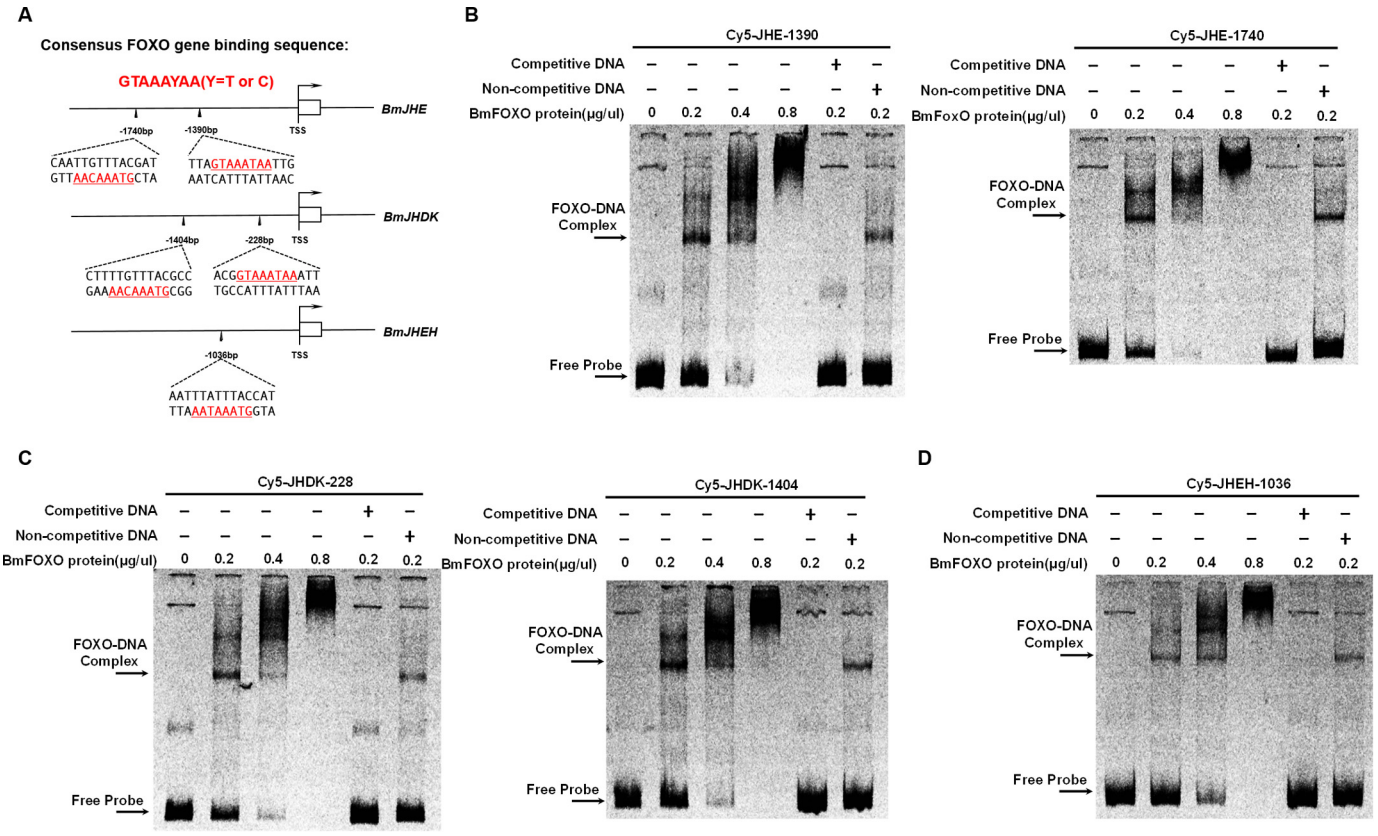

Figure 6. FOXO binds to conserved sequence in the promoters of genes coding for JH degradation enzymes. *A,* consensus FOXO-binding site sequence and potential binding sites in the promoter of *BmJHE*, *BmJHDK*, and *BmJHEH*. The *black line* indicates the genomic sequences of the three genes, and the *white box* and *arrow* show the first exon and transcription direction, respectively. The *filled black triangle* and *numbers below* (JHE, −1740 bp and −1390 bp; JHDK, −1404 bp and −228 bp; JHEH, −1036 bp) represent the distance between candidate FOXO-binding sites and TSS (transcription starting site). The sequence *under the dashed line* show the corresponding sequence (including the binding sequence), and the *underlined red letters* highlight the FOXO binding sequence. *B–D,* EMSA to test for binding of FOXO to the binding sites in the promoter regions of *JHE* (*B*), *JHDK* (*C*), and *JHEH* (*D*). Cy5-labeled oligos corresponding to the five sites (200–300 bp) were incubated with different concentrations (0, 0.2, 0.4, and 0.8 μg/μl) of purified FOXO protein. For competitive experiments, unlabeled or nonspecific DNA was added to the reaction mixture.

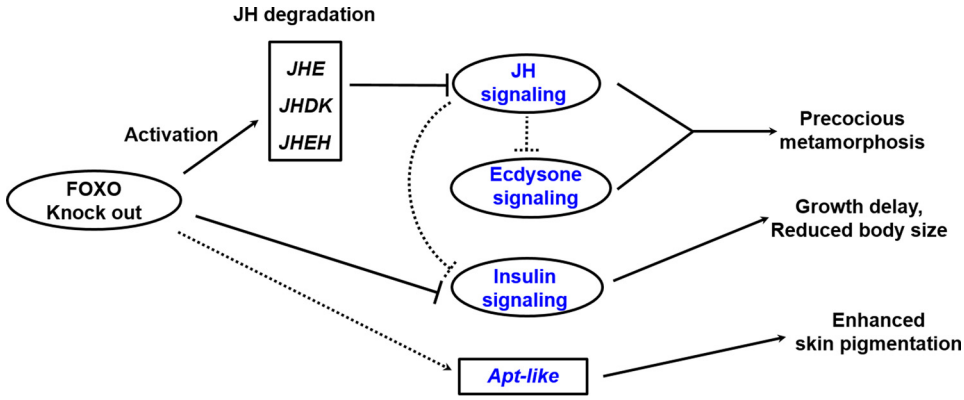

Figure 7. A model for the FOXO regulatory network for modulation of growth and development. Loss of function of FOXO activates JH degradation genes (*JHE*, *JHDK*, and *JHEH*) resulting in a reduction in JH titer. Lower levels of JH and/or FOXO further perturb ecdysone biosynthesis and action during the late larval stages (L3–L4) and induce the loss of fourth larval molt (trimolter). In FOXO knock-out silkworms, insulin signaling is also reduced, causing growth delay and reduced body size. Taken together, these findings show that FOXO plays a pivotal role in regulating growth and development through interactions with hormone signaling.

pathway and JH metabolism. Furthermore, the *BmFOXO* depletion trimolter is different from the previously reported JH-deficient mutants in *Bombyx* (32, 33), and the results suggested a more complex mechanisms, including IIS, JH, and ecdysone, are responsible for *BmFOXO*-induced precocious metamorphosis. The impaired insulin pathway, significant loss of JH, and perturbed ecdysone signaling resulted in skipping of the last molt and the maintenance of feeding until the larval-pupal transition. The major role of JH is to modulate ecdysone action (36), and inappropriate changes in JH titer can produce heterochronic shifts in the developmental program activated by ecdysone. Therefore, the activation of JH degradation by the *FOXO* mutation reduced the JH titer, which further altered ecdysone homeostasis and induced the loss of the fourth molt-

ing. Taken together, these results suggest a pivotal role for FOXO, which regulates insulin signaling and interacts with hormone signaling to control insect larval growth and development. With CA ceasing the production of JH during pupal commitment, the effect of FOXO mutation on JH metabolism was decayed and the ecdysone biosynthesis and action recovered, resulting in successful larval-pupal and pupal-adult metamorphosis.

The present study provides evidence that *BmFOXO* affects the JH degradation pathway, rather than the biosynthesis pathway, to regulate insect growth and development. The trimolter phenotype observed as a result of *BmFOXO* depletion is distinct from silkworm precocious metamorphosis induced by JH deficiency, indicating a more complex mechanism in which JH, IIS, and ecdysone are also involved (Fig. 7). As one of the downstream targets of IIS, FOXO is involved in comprehensive physiological processes, and its biological functions in insect growth and development remains to be fully elucidated.

Experimental procedures

Plasmid construction

The Cas9-expressing vector, *piggyBac[IE1-EGFP-nos-Cas9-SV40]* was constructed by inserting a Cas9 coding sequence, originating from PTD1-Cas9 (25), into *piggyBac[IE-EGFP-IE1-SV40]* with AatII and ApaI. Using the U6 promoter sequence as the template, the U6-sgRNA expressing sequence was obtained through two rounds of PCR with the primer U6-F: 5′-AGGTTATGTAGTACACATTG-3′ and the first-round reverse primers: FOXO-sgRNA-s1-R, 5′-TGCTATTTCTAGCTCTAAAACGCGGATGAATTGTTATCCCCACTTGTAGAGCACGATAT-3′ or FOXO-sgRNA-s2-R, 5′-TGCTATTTCTAGCTCTAAAACACGCCAAGCCCGGAAAATCCACTTGTAGAGCACGATAT-3′, and the second-round reverse primer: sgRNA-R, 5′-AAAAAAGCACCGACTCGGTGCCACTTTTTCAAGTTGATAACGGACTAGCCTTATTTTAACTTGCTATTTCTAGCTCTAAAAC-3′. The chained two U6-sgRNA expression cassettes were ligated using the Golden-Gate Assembly Kit (New England Biolabs) with the primers listed in supplemental Table S1. Subsequently, the expression unit was inserted into *piggyBac[IE1-DsRed2-SV40]* (37) with KpnI and ApaI to achieve the final construct *piggyBac[IE1-DsRed2-SV40-U6-FOXO-sgRNA(2×)]*. The plasmids were extracted using the Plasmid Midi Kit (Qiagen) according to the manufacturer's instructions and purified through phenol-chloroform treatment.

Insect strains and genetic transformation

The multivoltine and nondiapausing silkworm strain Nistari was used for genetic transformation (33) and phenotypic analysis in the present study. The DNA mixture was microinjected into preblastoderm G_0 embryos within 8 h after oviposition and incubated at 25 °C for 10–11 days until hatching. The larvae were reared with fresh mulberry leaves or artificial diets under standard conditions (33). G_0 adults mated with WT and G_1 offspring were screened under microscopy using RFP or GFP filters (Nikon AZ 100) to obtain positive transgenic animals.

Genotyping of target loci mutations

Genomic DNA were extracted after incubation with proteinase K (Thermo) and purified as previously described (38). The DNA fragments around the designed sgRNA targeting sites were amplified using Phusion Polymerase (New England Biolabs), and the corresponding PCR products were extracted and ligated into the pJET T-vector (Thermo) and subsequently sequenced. The Sanger sequencing results were analyzed and compared with those of the WT to confirm the detailed mutation events in FOXO mutants. For each sgRNA targeting site, at least 10 mono-clones were sequenced, and 3 different types of mutation events were demonstrated. The T7 endonuclease I assay was performed as previously reported (30).

Quantitative PCR

Two-step quantitative PCR was used to assay the related gene transcripts in transgenic *BmFOXO* mutants. Total RNA was extracted from different tissues at L4D2 or L4D3 (fat body for JH degradation, insulin, and 20E signaling-related genes, corpora allata for JH synthesis-associated genes, prothoracic gland for ecdysone synthesis-related genes) using TRIzol reagent (Invitrogen) and subsequently reverse-transcribed into cDNA using the RevertAid First-Strand cDNA synthesis kit (Thermo Fisher). The transcript levels were assayed using SYBR Green Master Mix (TOYOBO) via a standard curve normalized against *BmRP49* expression. The primers are listed in supplemental Table S2.

Electrophoretic mobility shift assay (EMSA)

The entire coding sequence for FOXO was obtained and cloned into the pET-32a expression vector (Thermo). Then, the pET-32a-FOXO-His vector was used to express FOXO protein in the JM110 *Escherichia coli* strain, followed by introduction with isopropyl 1-thio-β-D-galactopyranoside at 18 °C. Fusion FOXO protein was extracted and purified with nickel-nitrilotriacetic acid beads (Qiagen) according to the manufacturer's instructions. The predicted FOXO-binding sites containing DNA fragments were amplified using the primers listed in supplemental Table S2 comprising sequence-specific and Cy5-universal primer sequences (not labeled). Subsequently, labeled Cy5-tag universal primer was used to amplify the corresponding fragments, and the amplified fragments were collected using a Gel Extraction Kit (OMEGA). EMSA was performed using Cy5-labeled probes (Sangon) as previously described (39). For the competition assay, 100-fold excess of unlabeled DNA and nonspecific DNA were added as competitors. The mixture was electrophoresed at 4 °C on a 6% native polyacrylamide gel for 1.5 h at 100 V. The Cy5-labeled DNA on the gel was scanned and analyzed using the Starion FLA-9000 scanner (FujiFilm).

Hormone rescue experiments

For ecdysteroid rescue experiments, 5 μl of β-ecdysone (Sigma) (2 μg/μl, 10 μg in total) was injected into the first abdominal segment of each L4D3 FOXO-M larvae, and the same amount of 5% DMSO was injected as a control. The JH analog, methoprene (Sigma), was dissolved to 5 μg/μl in acetone and applied to the dorsum of newly molted fourth instar

FOXO mutant larvae (9–12 h after molting without feeding). Each larva was administered 2 μl of methoprene, and the same amount of acetone was used as a control. Twenty individuals were treated for each group.

Hormone titer measurement

Hemolymph (50–100 μl) was collected from L4D2 and L4D3 WT and FOXO mutant silkworms into tubes containing 5–10 μl of PTU (phenoloxidase inhibitor). The mixture was centrifuged, and the supernatant was recovered and transferred to a new tube for subsequent experiments.

20E titer measurement

The extracts were vacuum dried, re-dissolved in EIA buffer (Cayman), and subjected to enzyme immunoassay using the EIA kit (Cayman) to estimate the ecdysteroids titer as previously described (40, 41). The 20-hydroxyecdysone EIA antiserum, acetylcholinesterase (AchE)-linked 20E, and standard 20E (Sigma) were applied in competitive assays to determine 20E. The AchE activity was quantified using Ellman's reagent and measured at 410 nm using a Multiskan FC microplate photometer (Thermo).

Determination of JH titers

The concentration of JHI in the hemolymph was determined using LC-MS after derivatization as described by Furuta *et al.* (42). The minimum detection level of JH in the hemolymph was 0.5 pg/μl. Briefly, screw-top tubes containing 10 μl of internal standard (D_3-JHIII in toluene (50 pg/ml) was mixed with 1.5 ml of MeOH. To the internal standard solution, 50 μl of hemolymph was added and vortexed and mixed with 1.5 ml of 2% NaCl solution. The JHs were extracted three times with 0.5 ml of *n*-hexane and purified using a mini-column packed with aluminum oxide (activity III) to elute with 50% diethyl ether in *n*-hexane. After derivatization with MeOH to obtain methoxyhydrins of JH (JH-MHs), further purifications of the derivatives were performed using a aluminum oxide mini-column as describe above to elute with 50% ethyl acetate in *n*-hexane. The solvent was removed by a nitrogen gas stream of the traction, including the JH-MHs, and dissolved in acetonitrile. The HP1100MSD system was equipped with a 150 $\times$ 3-mm C_{18} reverse phase column (UG80; Shiseido) protected by a guard column using acetonitrile/distilled water (7:3, v/v) supplemented with 5 μM sodium acetate as the mobile phase at a flow rate of 0.4 ml/min. The selected ion groups (JHIII-MH+Na^+ as *m*/*z* 321.1 or 324.1 (D_3-internal standard), JHII-MH+Na^+ as *m*/*z* 335.1 and JHII-MH+Na^+ as *m*/*z* 349.1) were monitored. All determinations were performed in triplicate.

JHE enzymatic activity determination

JHE activity was determined using the method reported by McCutchen *et al.* (43) and described in detail by Tsubota *et al.* (21) using the substrate methyl 1-heptylthioacetothioate. For the assay, 5 μl of hemolymph collected from each larvae was added to 293 μl of assay buffer, *i.e.* 0.05 M sodium phosphate (pH 7.4) containing 0.025% of 5,5′-dithiobis(2-nitrobenzoic acid) (Nacalai Tesque) and 10% sucrose and preincubated at 25 °C for 10 min. Subsequently, 2 μl of 30 mM methyl 1-heptylthioacetothioate in EtOH was added, and the changes in absorbance at 405 nm were recorded on a microplate reader (Spectra-Max, Molecular Devices, Sunnyvale) for 5 min. The enzymatic activity was determined in triplicate.

RNA-seq analysis

Total RNA from fat bodies at L4D2 in WT and FOXO mutants was extracted and treated with DNase I to avoid genomic DNA contamination followed by purification using phenol/chloroform and dissolved in UltraPure distilled water (Invitrogen). The integrity of total RNA was evaluated using agarose electrophoresis. The RNA samples with high integrity were sent to BGI for RNA seq. The number and annotated information for the genes differentially expressed in WT and FOXO mutants were identified. The KEGG pathway and GO analyses were applied to summarize the pathways and processes showing gene expression changes.

Immunoblot analysis

Fat body homogenates from L4D3 of WT and FOXO-M larvae were dissolved in SDS-lysis buffer and centrifuged, supernatant were collected. The concentration of total protein was measured by BCA Protein Assay Kit (Thermo). Then, 30 μg of proteins were resolved by 12.5% SDS-PAGE and transferred to a PVDF membrane. The FOXO protein was detected with rabbit anti-FOXO primary antibody (1:1000 dilution, Youke) and alkaline phosphatase-conjugated goat anti-rabbit IgG (1:10,000 dilution, Youke) was applied as the secondary antibody. The ECL Plus Western blotting Detection Kit (GE Healthcare) was performed to detect the protein signal. The β-actin protein was treated as control.

Author contributions—B. Z., A. T., and Yongping Huang, conceived and designed the experiments. B. Z., Yuping Huang, T. S., and A. T. performed the experiments. B. Z., H. B., S. R. P., and A. T. analyzed the data. B. Z., Yuping Huang, J. X., T. S., and A. T. contributed reagents, materials, or analysis tools. B. Z., Yongping Huang, and A. T. wrote the paper.

References

1. Puig, O., Marr, M. T., Ruhf, M. L., and Tjian, R. (2003) Control of cell number by *Drosophila* FOXO: downstream and feedback regulation of the insulin receptor pathway. *Genes Dev.* **17,** 2006–2020
2. Puig, O., and Tjian, R. (2005) Transcriptional feedback control of insulin receptor by dFOXO/FOXO1. *Genes Dev.* **19,** 2435–2446
3. Daimon, T., Uchibori, M., Nakao, H., Sezutsu, H., and Shinoda, T. (2015) Knockout silkworms reveal a dispensable role for juvenile hormones in holometabolous life cycle. *Proc. Natl. Acad. Sci. U.S.A.* **112,** E4226–E4235
4. Mirth, C. K., Tang, H. Y., Makohon-Moore, S. C., Salhadar, S., Gokhale, R. H., Warner, R. D., Koyama, T., Riddiford, L. M., and Shingleton, A. W. (2014) Juvenile hormone regulates body size and perturbs insulin signaling in *Drosophila*. *Proc. Natl. Acad. Sci. U.S.A.* **111,** 7018–7023
5. Colombani, J., Bianchini, L., Layalle, S., Pondeville, E., Dauphin-Villemant, C., Antoniewski, C., Carré, C., Noselli, S., and Léopold, P. (2005) Antagonistic actions of ecdysone and insulins determine final size in *Drosophila*. *Science* **310,** 667–670
6. Mirth, C., Truman, J. W., and Riddiford, L. M. (2005) The role of the prothoracic gland in determining critical weight for metamorphosis in *Drosophila melanogaster*. *Curr. Biol.* **15,** 1796–1807

7. Delanoue, R., Slaidina, M., and Léopold, P. (2010) The steroid hormone ecdysone controls systemic growth by repressing dMyc function in *Drosophila* fat cells. *Dev. Cell* **18,** 1012–1021
8. Verdu, J., Buratovich, M. A., Wilder, E. L., and Birnbaum, M. J. (1999) Cell-autonomous regulation of cell and organ growth in *Drosophila* by Akt/PKB. *Nat. Cell Biol.* **1,** 500–506
9. Brogiolo, W., Stocker, H., Ikeya, T., Rintelen, F., Fernandez, R., and Hafen, E. (2001) An evolutionarily conserved function of the *Drosophila* insulin receptor and insulin-like peptides in growth control. *Curr. Biol.* **11,** 213–221
10. Böhni, R., Riesgo-Escovar, J., Oldham, S., Brogiolo, W., Stocker, H., Andruss, B. F., Beckingham, K., and Hafen, E. (1999) Autonomous control of cell and organ size by CHICO, a Drosophila homolog of vertebrate IRS1–4. *Cell* **97,** 865–875
11. Tu, M. P., Yin, C. M., and Tatar, M. (2005) Mutations in insulin signaling pathway alter juvenile hormone synthesis in *Drosophila melanogaster*. *Gen. Comp. Endocrinol.* **142,** 347–356
12. Carter, M. E., and Brunet, A. (2007) FOXO transcription factors. *Curr. Biol.* **17,** R113–R114
13. Calnan, D. R., and Brunet, A. (2008) The FoxO code. *Oncogene* **27,** 2276–2288
14. Hwangbo, D. S., Gersham, B., Tu, M. P., Palmer, M., and Tatar, M. (2004) *Drosophila* dFOXO controls lifespan and regulates insulin signalling in brain and fat body. *Nature* **429,** 562–566
15. Giannakou, M. E., Goss, M., Jünger, M. A., Hafen, E., Leevers, S. J., and Partridge, L. (2004) Long-lived *Drosophila* with overexpressed dFOXO in adult fat body. *Science* **305,** 361
16. Lin, K., Dorman, J. B., Rodan, A., and Kenyon, C. (1997) daf-16: an HNF-3/forkhead family member that can function to double the life-span of *Caenorhabditis elegans*. *Science* **278,** 1319–1322
17. Lehtinen, M. K., Yuan, Z., Boag, P. R., Yang, Y., Villén, J., Becker, E. B., DiBacco, S., de la Iglesia, N., Gygi, S., Blackwell, T. K., and Bonni, A. (2006) A conserved MST-FOXO signaling pathway mediates oxidative-stress responses and extends life span. *Cell* **125,** 987–1001
18. Jünger, M. A., Rintelen, F., Stocker, H., Wasserman, J. D., Végh, M., Radimerski, T., Greenberg, M. E., and Hafen, E. (2003) The *Drosophila* forkhead transcription factor FOXO mediates the reduction in cell number associated with reduced insulin signaling. *J. Biol.* **2,** 20
19. Kramer, J. M., Davidge, J. T., Lockyer, J. M., and Staveley, B. E. (2003) Expression of *Drosophila* FOXO regulates growth and can phenocopy starvation. *BMC Dev. Biol.* **3,** 5
20. Slack, C., Giannakou, M. E., Foley, A., Goss, M., and Partridge, L. (2011) dFOXO-independent effects of reduced insulin-like signaling in *Drosophila*. *Aging Cell* **10,** 735–748
21. Tsubota, T., Nakakura, T., Shinoda, T., and Shiotsuki, T. (2010) Characterization and analysis of novel carboxyl/cholinesterase genes possessing the Thr-316 motif in the silkworm, *Bombyx mori*. *Biosci. Biotechnol. Biochem.* **74,** 2259–2266
22. Rauschenbach, I. Y., Karpova, E. K., and Gruntenko, N. E. (2015) dFOXO transcription factor regulates juvenile hormone metabolism in *Drosophila melanogaster* females. *Genetika* **51,** 1083–1086
23. Süren-Castillo, S., Abrisqueta, M., and Maestro, J. L. (2012) FoxO inhibits juvenile hormone biosynthesis and vitellogenin production in the German cockroach. *Insect Biochem. Mol. Biol.* **42,** 491–498
24. Hossain, M. S., Liu, Y., Zhou, S., Li, K., Tian, L., and Li, S. (2013) 20-Hydroxyecdysone-induced transcriptional activity of FoxO up-regulates brummer and acid lipase-1 and promotes lipolysis in *Bombyx* fat body. *Insect Biochem. Mol. Biol.* **43,** 829–838
25. Wang, Y., Li, Z., Xu, J., Zeng, B., Ling, L., You, L., Chen, Y., Huang, Y., and Tan, A. (2013) The CRISPR/Cas system mediates efficient genome engineering in *Bombyx mori*. *Cell Res.* **23,** 1414–1416
26. Daimon, T., Kiuchi, T., and Takasu, Y. (2014) Recent progress in genome engineering techniques in the silkworm, *Bombyx mori*. *Dev. Growth Differ* **56,** 14–25
27. Li, Z., You, L., Zeng, B., Ling, L., Xu, J., Chen, X., Zhang, Z., Palli, S. R., Huang, Y., and Tan, A. (2015) Ectopic expression of ecdysone oxidase impairs tissue degeneration in *Bombyx mori*. *Proc. Biol. Sci.* **282,** 20150513
28. Xu, J., Chen, S., Zeng, B., James, A. A., Tan, A., and Huang, Y. (2017) *Bombyx mori* P-element somatic inhibitor (BmPSI) is a key auxiliary factor for silkworm male sex determination. *PLoS Genet.* **13,** e1006576
29. Kondo, S., and Ueda, R. (2013) Highly improved gene targeting by germline-specific Cas9 expression in *Drosophila*. *Genetics* **195,** 715–721
30. Zeng, B., Zhan, S., Wang, Y., Huang, Y., Xu, J., Liu, Q., Li, Z., Huang, Y., and Tan, A. (2016) Expansion of CRISPR targeting sites in *Bombyx mori*. *Insect Biochem. Mol. Biol.* **72,** 31–40
31. Dubrovsky, E. B. (2005) Hormonal cross talk in insect development. *Trends Endocrinol. Metab.* **16,** 6–11
32. Daimon, T., Kozaki, T., Niwa, R., Kobayashi, I., Furuta, K., Namiki, T., Uchino, K., Banno, Y., Katsuma, S., Tamura, T., Mita, K., Sezutsu, H., Nakayama, M., Itoyama, K., Shimada, T., and Shinoda, T. (2012) Precocious metamorphosis in the juvenile hormone-deficient mutant of the silkworm, *Bombyx mori*. *PLoS Genet.* **8,** e1002486
33. Tan, A., Tanaka, H., Tamura, T., and Shiotsuki, T. (2005) Precocious metamorphosis in transgenic silkworms overexpressing juvenile hormone esterase. *Proc. Natl. Acad. Sci. U.S.A.* **102,** 11751–11756
34. Herold, M. J., Rohrbeck, L., Lang, M. J., Grumont, R., Gerondakis, S., Tai, L., Bouillet, P., Kaufmann, T., and Strasser, A. (2013) Foxo-mediated Bim transcription is dispensable for the apoptosis of hematopoietic cells that is mediated by this BH3-only protein. *EMBO Rep.* **14,** 992–998
35. Niwa, R., Namiki, T., Ito, K., Shimada-Niwa, Y., Kiuchi, M., Kawaoka, S., Kayukawa, T., Banno, Y., Fujimoto, Y., Shigenobu, S., Kobayashi, S., Shimada, T., Katsuma, S., and Shinoda, T. (2010) Non-molting glossy/shroud encodes a short-chain dehydrogenase/reductase that functions in the "Black Box" of the ecdysteroid biosynthesis pathway. *Development* **137,** 1991–1999
36. Riddiford, L. M., Hiruma, K., Zhou, X., and Nelson, C. A. (2003) Insights into the molecular basis of the hormonal control of molting and metamorphosis from *Manduca sexta* and *Drosophila melanogaster*. *Insect Biochem. Mol. Biol.* **33,** 1327–1338
37. Li, Z., Zeng, B., Ling, L., Xu, J., You, L., Aslam, A. F., Tan, A., and Huang, Y. (2015) Enhancement of larval RNAi efficiency by over-expressing argonaute2 in *Bombyx mori*. *Int. J. Biol. Sci.* **11,** 176–185
38. Ling, L., Ge, X., Li, Z., Zeng, B., Xu, J., Aslam, A. F., Song, Q., Shang, P., Huang, Y., and Tan, A. (2014) MicroRNA Let-7 regulates molting and metamorphosis in the silkworm, *Bombyx mori*. *Insect Biochem. Mol. Biol.* **53,** 13–21
39. Zhang, L., Nie, X., Ravcheev, D. A., Rodionov, D. A., Sheng, J., Gu, Y., Yang, S., Jiang, W., and Yang, C. (2014) Redox-responsive repressor Rex modulates alcohol production and oxidative stress tolerance in *Clostridium acetobutylicum*. *J. Bacteriol.* **196,** 3949–3963
40. Kingan, T. G., and Adams, M. E. (2000) Ecdysteroids regulate secretory competence in Inka cells. *J. Exp. Biol.* **203,** 3011–3018
41. Gelman, D. B., Blackburn, M. B., and Hu, J. S. (2002) Timing and ecdysteroid regulation of the molt in last instar greenhouse whiteflies (*Trialeurodes vaporariorum*). *J. Insect Physiol.* **48,** 63–73
42. Furuta, K., Ichikawa, A., Murata, M., Kuwano, E., Shinoda, T., and Shiotsuki, T. (2013) Determination by LC-MS of juvenile hormone titers in hemolymph of the silkworm, *Bombyx mori*. *Biosci. Biotechnol. Biochem.* **77,** 988–991
43. McCutchen, B. F., Szekacs, A., Huang, T. L., Shiotsuki, T., and Hammock, B. D. (1995) Characterization of a spectrophotometric assay for juvenile hormone esterase. *Insect Biochem. Mol. Biol.* **25,** 119–126

The FOXO transcription factor controls insect growth and development by regulating juvenile hormone degradation in the silkworm, *Bombyx mori*

Baosheng Zeng, Yuping Huang, Jun Xu, Takahiro Shiotsuki, Hua Bai, Subba Reddy Palli, Yongping Huang and Anjiang Tan

J. Biol. Chem. 2017, 292:11659-11669.
doi: 10.1074/jbc.M117.777797 originally published online May 10, 2017